Annals of Biomedical Engineering, Vol. 36, No. 3, March 2008 (© 2008) pp. 513–521
DOI: 10.1007/s10439-008-9439-6

Residual Stress Patterns Affect Cell Distributions on Injection-Molded Poly-L-Lactide Substrate

SHENG-YANG LEE,[1] HOW TSENG,[2] KENG-LIANG OU,[3] JEN-CHANG YANG,[3] KUO-NING HO,[1] CHE-TONG LIN,[1] and HAW-MING HUANG[3]

[1]School of Dentistry, Taipei Medical University, 250, Wu-Hsing Street, Taipei, Taiwan; [2]Graduate Institute of Medical Sciences, Taipei Medical University, 250, Wu-Hsing Street, Taipei, Taiwan; and [3]Graduate Institute of Biomedical Materials & Engineering, Taipei Medical University, 250, Wu-Hsing Street, Taipei, Taiwan

(Received 21 October 2007; accepted 10 January 2008; published online 19 January 2008)

Abstract—The effects of residual intra-substrate stress distribution on cell behavior have not been systematically investigated. Thus, the objective of this research was to analyze the relationship between cell distribution and internal stress patterns. A photoelastic method was used for residual stresses identification. Poly-L-lactide (PLLA) discs were prepared using an injection molding technique. MG-63 and NIH-3T3 cells were cultured on the surface of the PLLA disc. The cell distributions for high and low-stress regions were measured and compared. There were significantly more cells in the low-stress regions relative to high-stress analogs ($p < 0.05$). Further, linear relationships were demonstrated for both MG-63 and NIH-3T3 models with high correlation coefficients of 0.80 and 0.95, respectively. These results suggest that the distribution of residual stress in substrates affect cell behavior. These findings may provide greater insight into the interaction between cells and substrates, and may serve as a useful reference in future clinical study.

Keywords—Residual stress, Poly-L-lactide, Mechanical sensing, Osteoblast.

INTRODUCTION

Tissue engineering is a remodeling technique utilizing artificial scaffolding. Its success greatly depends on the interactions between the cells and the chemical and physical environments of the entraining biomaterials. The physical effects at the cell–environment interface can now be understood using mechanobiology, which offers a theoretical basis for mechanical force-influenced bone remodeling.[29,31]

Many studies have demonstrated that cells not only respond to mechanical forces but also react to the surface properties of scaffolds. For example, substrate rigidity reportedly plays a crucial role in cellular attachment,[5] migration,[14] morpholog,[27] proliferation,[30] and cytoskeleton expression.[5,10] In addition, the crystallinity, roughness and porosity of polymeric substrates affect the behavior of various cell types.[11,15,19,27,32,36]

Residual stress is the stress that persists after manufacture despite the subsequent absence of the initial loading. It is an important physical property of biomaterials, influencing their mechanical performance in the human body. As residual stress also exist in human arteries, heart muscle, skin, and bone,[3,20,22,28] it should be considered when analyzing the mechanical performance of such tissues.

When cutting and injection molding are used in the manufacture of a scaffold or fixation device, uncontrolled residual stresses develop inside the materials. In general, uncontrolled residual stress reduces the mechanical performance of the device. However, it was reported that residual stresses in biomaterials have biological effects on the strain-induced function of mechanosensing cells.[26] For example, due to these mechanosensing properties, residual stress can provide a mechanical stimulator for bone remodeling.[28] Since various stress-induced strain parameters, including strain energy density, maximal principal strain, and volumetric strain, have effects on bone structure,[23] residual strain in scaffolds may subsequently affect cellular growth behavior. However, although many studies have demonstrated that the mechanical environment plays an important role in regulating cell behavior, the specific role of residual stress/strain was not systematically discussed.

Recently, poly-L-lactide (PLLA), which was developed for use in cell culture studies, has become the most popular bioresorbable material for fixation or scaffolding because of its controlled physical and chemical surface properties.[15,32] It has been demonstrated that the interaction between cells and the

Address correspondence to Haw-Ming Huang, Graduate Institute of Biomedical Materials & Engineering, Taipei Medical University, 250, Wu-Hsing Street, Taipei, Taiwan. Electronic mail: hhm@tmu.edu.tw

PLLA substrate was affected by its chemical composition, crystallinity, topography, porosity, and surface energy.[1,13,17] However, to discover why cells are responsive to differences between various mechanical environments, it is necessary to culture cells on substrates with different physical properties while keeping the chemical properties of the surface constant.

MG-63 cells were originally derived from a human osteogenic sarcoma. It was subsequently found that its physiology is dependent on surface topography of PLLA.[13,37] The NIH-3T3 fibroblast is a continuous cell line established from Swiss mouse embryo. Several investigations have demonstrated that the movement, shape, growth rate, adhesion, and cytoskeletal expression of these cells are affected by the stiffness, rigidity, and morphology of the substrates.[4,14,33] To test the hypothesis that residual stresses of biomaterial also affect cell behavior, we cultured MG-63 and NIH-3T3 cells on PLLA discs with residual stress gradients but without variation in the chemical properties of the disc surface. A photoelastic technique was used to monitor the residual stress patterns of the PLLA substrates due to its excellent property in optical birefringence. The effects of residual stress patterns on cellular distribution could then be compared.

EXPERIMENTAL

PLLA Sample Preparation

Prior to processing, PLLA chips with molecular weight of 140 kDa (lot# 020301; BioTech One Ltd., Taipei, Taiwan) were vacuum-dried at 70 °C overnight to ensure a moisture content below 250 ppm. All disc-shape specimens (14-mm diameter, 1-mm thickness), with a circular mark, a location of ejector pin, (6-mm diameter, 0.05 mm height) on the reverse side were manufactured at 185 °C using an automatic injection-molding machine (Fig. 1) in a clean room (class 10,000). Typical molding conditions are listed in Table 1. In each test disc, the area of the circle marker was divided into nine squares (Fig. 2a). Five square regions, labeled left (LR), central (CR), right (RR), central-up (CUR), and central-low regions (CLR), were used for analysis.

TABLE 1. Temperature setting of the injection-molding process.

Zone	Barrel temperature setting (°C)
Feed throat	25
Feed section	170
Compression section	175
Metering section	180
Hot runner	185
Nozzle tips	185

Wide-Angle X-ray Diffraction (WAXRD)

The WAXRD experiments were performed by an X-ray diffractometer (D/MAX 2000 PC, Rigaku Co., Tokyo, Japan) in reflection mode to determine the crystalline properties in all five square regions of each PLLA specimen. The X-ray generator was operated at 30 KV and 20 mA with Ni-filtered CuKα (1.54 Å) radiation. The WAXRD 2θ scans were acquired at a rate of 2°/min ranged between 10 and 40°.

Surface Roughness Measurement

Surface roughness at various test regions was measured using scanning topography measurement (STM; Talyscan 150, Taylor Hobson Ltd., Leicester, GB) with a diamond-stylus inductive gage (2-μm tip radius, 90° tip angle) for contact measurement. An area (0.5×0.5 mm^2) in each region was moved on the stage to scan the complete measurement areas. Each profile was recorded at a resolution of 1 μm. The roughness

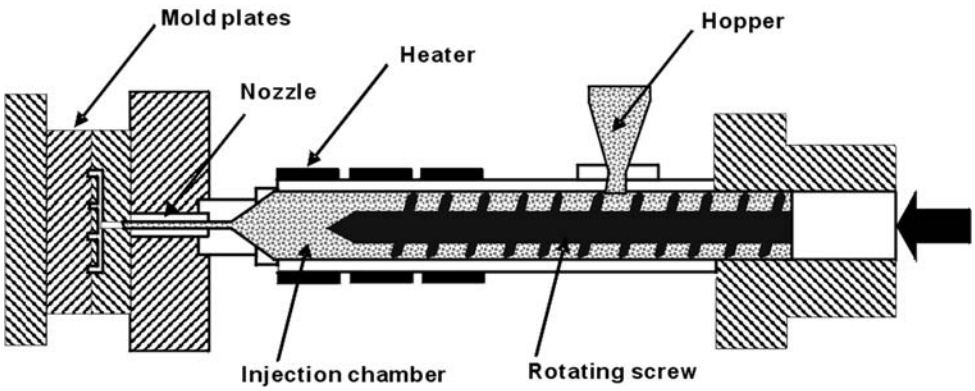

FIGURE 1. Injection molds for fabrication of PLLA discs.

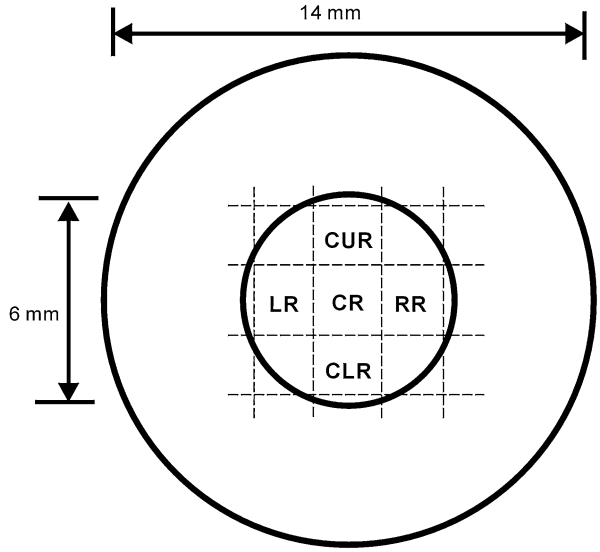

FIGURE 2. Geometry of injected PLLA disc. The circular marker was divided into nine squares. LR, CR, RR, CUR, and CLR are the left, central, right, central-up, and central-low regions, respectively.

(Sz) was defined as the length of vertical movement of the gage.

Photoelastic Analysis

Residual stress in thermosetting polymers can be detected by measuring optical birefringence patterns using polarization.[25] In this study, photoelastic analysis, based on optical birefringence theory, was conducted to examine the residual stress distributions in the injection-molded PLLA discs. Before cell culture, all PLLA discs were examined in the field of a custom-designed circular polariscope (Fig. 3). The sample was located between a pair of polarizing filters labeled as polarizer and analyzer. The polarization axis of the polarizer and analyzer was arranged so that the filters were orthogonal with respect to each other. A white light source was employed to facilitate isochromatic fringe observation, as described previously.[25,34] The white light produced stress patterns of colored fringes throughout the test discs. The isochromatic fringe patterns were photographed using a digital camera (Coolpix 4500; Nikon Co., Tokyo, Japan) and then transferred to a computer, where quantification of the fringe orders was performed. High residual stress areas were indicated by numerous surrounding lines. Mechanically, the fringe order at any point on the model has been established, it is possible to compute principle stress differences using the stress-optical law:

$$\sigma_1 - \sigma_2 = \frac{Nf_\sigma}{h}$$

where σ_1 and σ_2 are the principle stresses in the plane of the model; N and h are fringe order and sample thickness, respectively; and, f_σ is an optical constant of the model material for a given wavelength. According to the mechanical principle, the maximum shear stress at each location can be given by:

$$\tau_{\max} = \frac{1}{2}(\sigma_1 - \sigma_2) = \frac{Nf_\sigma}{2h}$$

In this study, the thickness and material constant of all the injection-molded PLLA samples are the same. That is, the fringe order of a sample is proportional to the maximum internal shear stress. We recorded color patterns caused by residual shear stress distributions at each location, and converted them to fractional fringe order (N) according to a color-fringe order conversion table.[8] The fringe order of each square region was obtained by averaging the measured values at the left and right margins of the square.

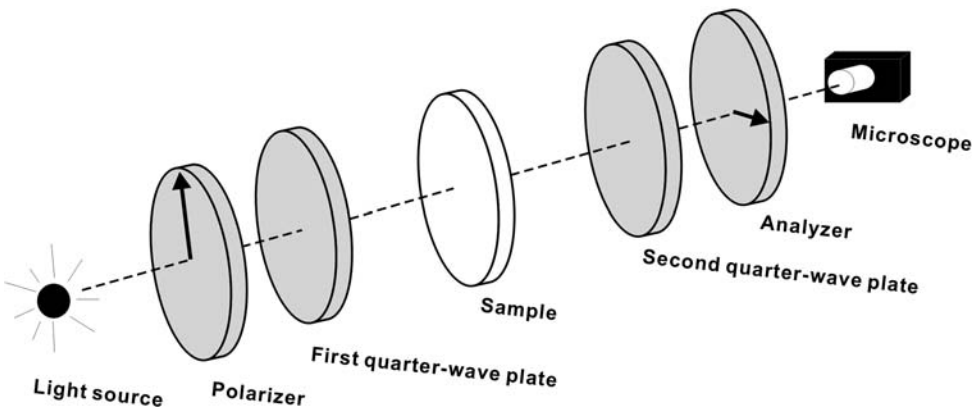

FIGURE 3. Block diagram of optical-component arrangement and axis orientation of the circular polariscope used for photoelastic analysis.

In vitro Cell Culture

Both MG-63 osteoblast-like cells [ATCC CRL-1427] and NIH-3T3 fibroblast analogs [ATCC CRL-1658] were used in this study. Mechanosensing characteristics have been demonstrated for both cell types in cell culture experiments.[24,30] The test cells were seeded into Petri dishes (Nunclon; Nunc, Roskilde, Denmark) at a density of 10,000 cells/mL, and maintained in Dulbecco's modified Eagle's medium (DMEM; HyClone, Utah, USA) supplemented with L-glutamine (4 mM), 10% fetal bovine serum (FBS), and 1% penicillin–streptomycin. Cell cultures were incubated in 5% CO_2 at 37 °C and 100% humidity.

To test the growth differences between tissue-cultured plate (TCP) and PLLA disc, cell viability was detected every 24 h. At each observation time, the cells were incubated with a tetrazolium salt, MTT, as per supplier instructions (MTT kit; Roche Applied Science, Mannheim, Germany). After addition of the colorometric substrate for 4 h, the viable cells convert MTT salt to a water-insoluble formazan dye, which can be quantitated after solubilization with 500 μL DMASO for 5 min using a microplate reader (Model 2020; Anthos Labtec Instruments, Wals, Austria) at 570/690 nm. The absorbance directly correlates with the cell number.

Scanning Electron Microscopy

Scanning electron microscopy (SEM) was used to compare topographical and morphological variations between high and low residual-stress regions on the PLLA discs. At 48 h, the culture media were removed and the samples rinsed three times with PBS before fixation in 2.5% glutaraldehyde and 2% paraformaldehyde for 20 min and then 1% osmium tetroxide in 0.1 mol/L PBS for 30 min. After the initial fixation, the samples were rinsed and postfixed in 1% osmium tetroxide for 1 h. Samples were subsequently washed with PBS and dehydrated in an ethanol series (70, 80, 90, 95, and 100%) in a critical point dryer (HCP-2; Hitachi Ltd, Chiyoda, Tokyo, Japan). A thin layer of palladium gold was coated onto the samples using a sputtering apparatus (IB-2; Hitachi Ltd, Chiyoda, Tokyo, Japan) before the morphological features of the cells and disc surfaces were examined using a Hitachi S-2400 electron microscope (Hitachi Ltd., Chiyoda, Tokyo, Japan).

Cell Enumeration

To test the effects of residual stress on cellular behavior, the cells were cultured on the smooth and textured surface of the PLLA disc. The prepared PLLA discs were placed in 24-well polystyrene tissue-culture plates. Cells with a density of 5000 cells/mL (in 250 mL cultured medium) were carefully seeded on the center of the PLLA surface. After the cells were attached to the PLLA surfaces, an additional 250 mL of cultured medium was added in the cultured wells. At 48 h, cell distributions on the PLLA surface were recorded using an inverted microscope (Eclipse TS100l Nikon Co., Tokyo, Japan) interfaced with a digital camera (Coolpix 4500; Nikon Co., Tokyo, Japan), with the cells (400×) in the circle marker reconstructed using image processing. Cell numbers in regions LR, CR, RR, CUR, and CLR were counted using commercial cell-counting software (Image-pro Plus; Media Cybenetics Inc., Silver Spring, MD). In this study, cell distribution was defined as the ratio between the number of cells in a specific region relative to the total for the five defined regions. Three independent experiments were performed for all tests. In each experiment, data are presented as mean ± standard deviation (SD) with four samples. Differences in cell distribution between various regions were compared using Student's *t*-test. Probability values less than 0.05 were considered significant.

RESULTS

Surface Topographical Description

The roughness (Sz) measurements for LR, CR, RR, CUR, and CLR are 2.37 ± 0.0.88, 2.57 ± 0.45, 2.27 ± 0.88, 2.66 ± 0.59, and 2.48 ± 0.53 μm, respectively. Statistical analysis failed to demonstrate significant difference comparing the roughness values for the five regions. WAXRD tests showed that the PLLA samples manufactured in this study had an amorphous structure. The X-ray diffraction pattern samples of the injection-molded disc (Fig. 4) showed

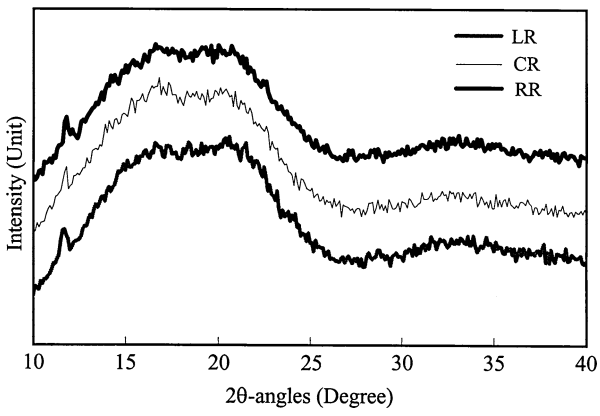

FIGURE 4. Typical samples of X-ray spectra for PLLA disc measured at LR, CR, and RR; no obviously crystallinity peaks are evident.

no obvious diffraction peak, revealing that the injection molded PLLA sample had an amorphous structure. Furthermore, the microstructure and crystallinity have no difference as comparing the diffraction patterns of the five regions.

Residual Stresses Detection of PLLA

Photoelastic analysis was used to assess the residual stresses in the injection molded PLLA, with the stress patterns highly consistent comparing the independent samples. There was zero variation in fringe order comparing the four test discs. The highest residual stress was observed at the injection port (black arrow in Fig. 5a), with the black zero-order fringes usually locating at the opposite boundary. Apart form the injection port, high residual stresses were concentrated close to the left boundary of the circle marker. Converting the color patterns to fringe order revealed the most stress-free area at the right region of the test disc. The color pattern of this region, orange (equivalent of 0.8 fringe order) at the right margin and blue-green (equivalent of a 1.22 fringe order) at the left margin (blue arrow in Fig. 5b), is counted as 1.08. Further, the largest fringe order, with a value of 2.75, was found at the left region (red arrow in Fig. 5b).

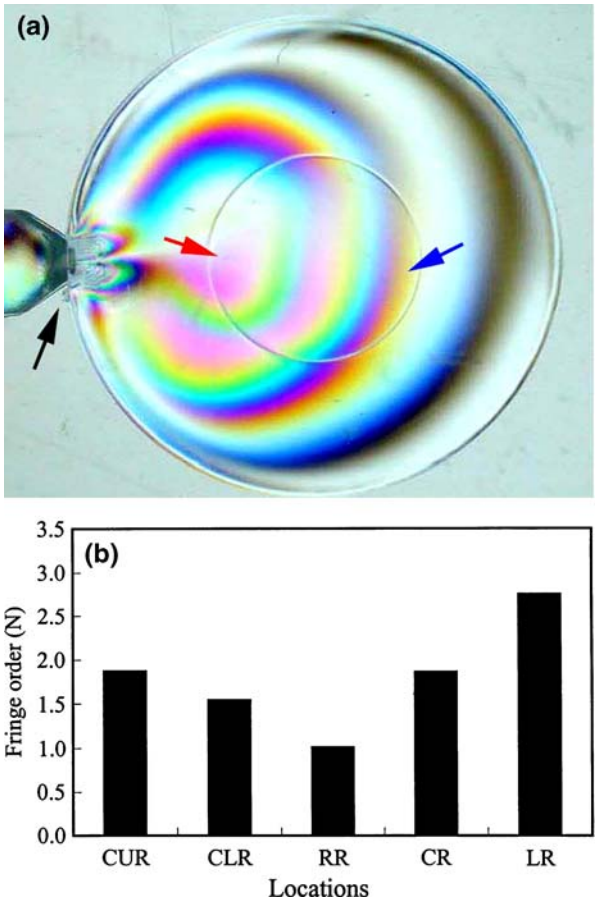

FIGURE 5. (a) Isochromatic fringe patterns of PLLA disc; (b) fringe order of each region was converted from color pattern. The black arrow indicates injection port. Red and blue arrows indicate the areas (in the circle marker) with highest and lowest residual stress, respectively.

Cell Distributions

The cells cultured on the PLLA substrates with lower residual stresses had higher cell distributions (Fig. 6). There were significantly more MG-63 cells at RR (23.68 ± 2.88%) compared to CR (15.89 ± 1.50%) and LR (15.15 ± 1.96%) ($p < 0.01$). NIH-3T3 cell distributions at RR (25.22 ± 2.78%) was 1.26 and 1.57-fold higher compared to CR ($p < 0.05$) and LR ($p < 0.01$), respectively. No such differences were demonstrated, however, comparing the cell distributions at CUR and CLR. When the fringe order values at various regions on the test discs were plotted against their corresponding cell distributions, linear relationships were found for both MG-63 and NIH-3T3 models (Figs. 7a and 7b, respectively). The correlation coefficient for the MG-63 cells ($R = 0.80$, $p < 0.05$) is slightly lower than the NIH-3T3 analogs ($R = 0.95$, $p < 0.05$).

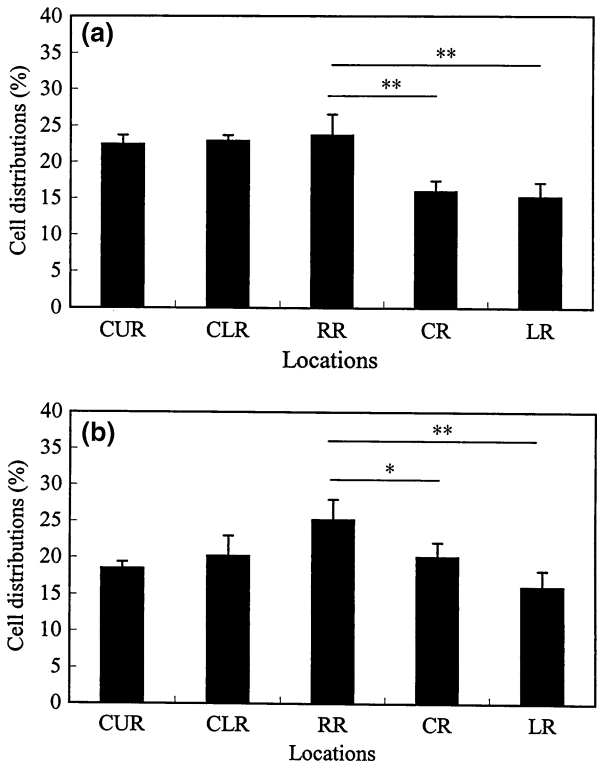

FIGURE 6. Distribution of MG-63 (a) and NIH-3T3 (b) cells at various regions. '*' and '' denote $p < 0.05$ and 0.01, respectively ($n = 4$ cultures).**

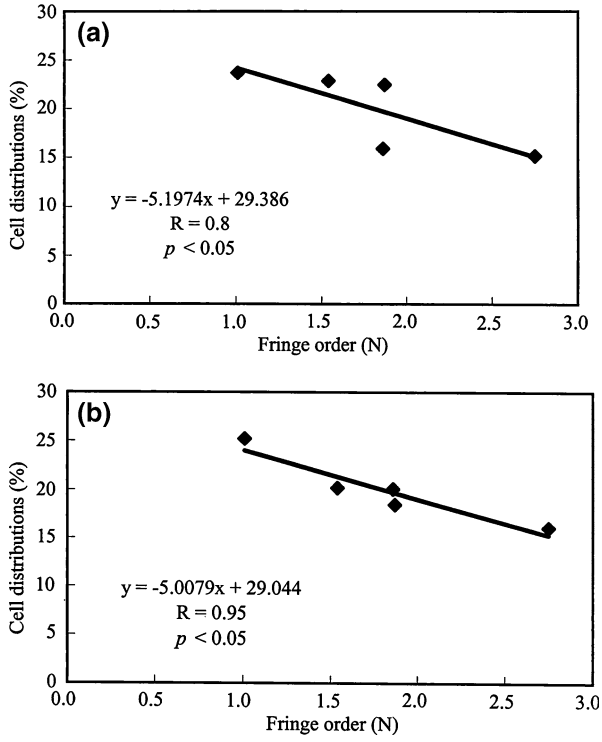

FIGURE 7. Relationship between mean cell distribution and fringe order value for MG-63 (a) and NIH-3T3 cells (b). Solid lines represent best-fit linear regression.

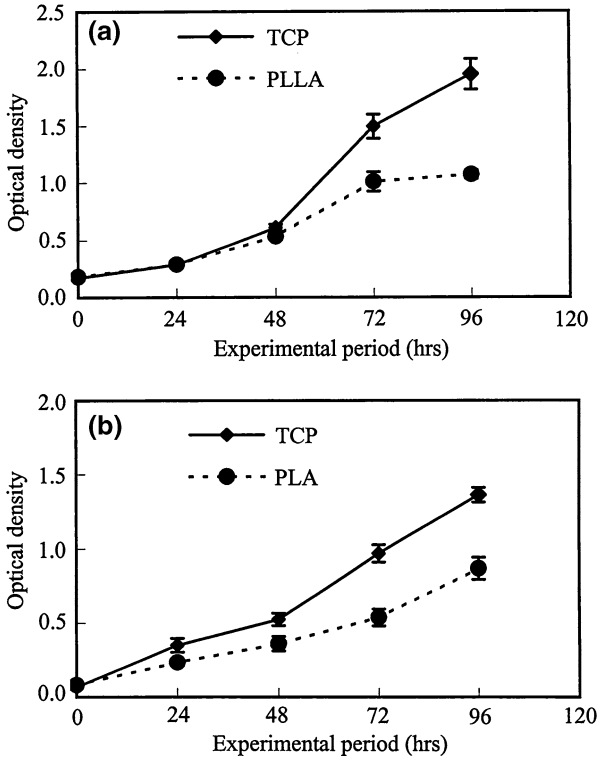

FIGURE 8. Growth curves for MG-63 and NIH-3T3 cells on tissue culture plate (a) and PLLA disc (b) for 96 h (n = 4 cultures).

Cell Proliferation

MG-63 and NIH-3T3 cells were cultured on TCP and PLLA substrates for 96 h (Fig. 8). Statistically significant differences in MTT counts were not demonstrated for any of the observation intervals before the 48-h period comparing the MG-63 cells cultured on the TCP and PLLA substrates. However, after 48 h, the cells cultured on the PLLA substrates had a significant decrease in proliferation rate relative to the TCP substrates, with a maximum 1.8-fold differences at 96 h (Fig. 8a) ($p < 0.05$). In the NIH-3T3 experiments, a significant decreased in proliferation rate of PLLA group cells was first noted at 24 h. At 96 h, the cell counts of the TCP group were 1.57-fold higher than the PLLA group (Fig. 8b).

Cell Morphology

The SEM images acquired at 48 h show distinct morphological differences between MG-63 and NIH-3T3 cells. The MG-63 cells changed from polygonal into more stellar shapes with abundant extensive processes contacting with each other. However, no obvious differences in cellular morphology can be identified between LR (high residual stress) and RR (low residual stress) groups (Figs. 9a and 9b). The NIH-3T3 cells were evenly distributed and appeared to form a relatively thin, continuous monolayer (Figs. 9c and 9d). However, there appeared to be no differences in cellular morphology across regions. Furthermore, when comparing the topographic characteristics of PLLA surfaces between LR and RR, no obvious differences were found for both the two cell culture models (Fig. 9).

DISCUSSION

Injection molding is widely used for rapid production of thermoplastic devices with complex geometric shapes. The complete process of injection molding consists of three stages: filling, packing and cooling. In the last stage, the PLLA melt continues to cool inwards from the cold mold surface toward the center of the molded sample. This nonuniform cooling process results in high flow stresses, causing the PLLA molecules to become oriented in the direction of flow. These shear stresses are frozen in the molded PLLA and cannot relax. Since the molecular backbone of the injection-molded PLLA has different orientations, the polymer will demonstrate anisotropic optical polarizability. Shindo *et al.*, measured the optical properties of cast-molded polymer and found that cooling speed

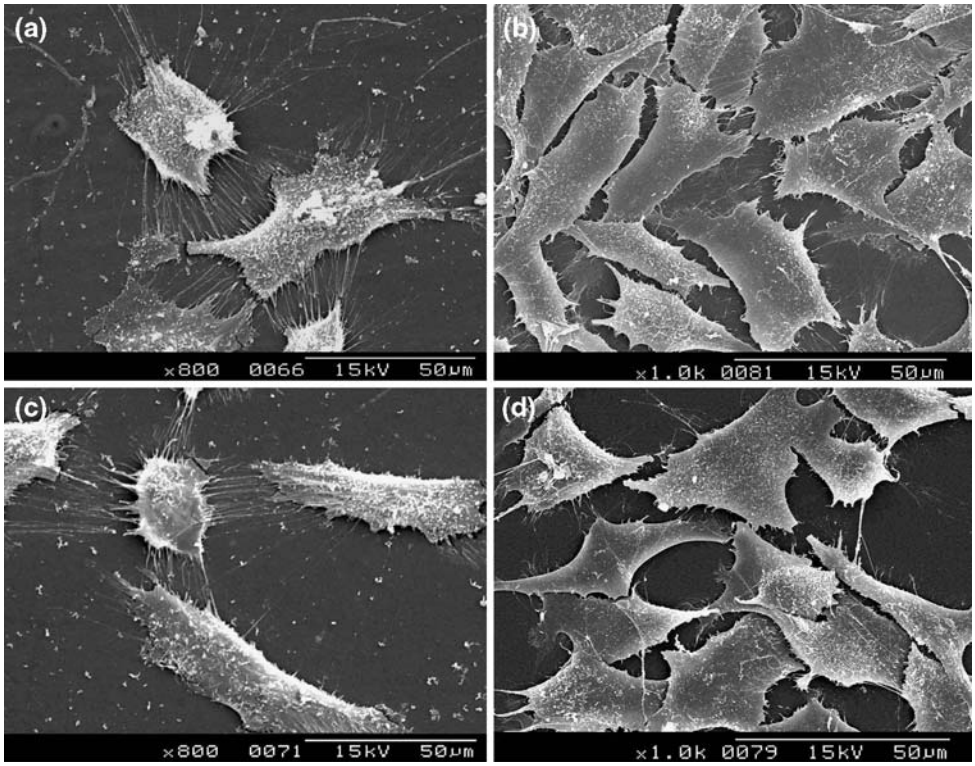

FIGURE 9. Scanning electron microscopy images of cells cultured on left (a, c) and right (b, d) regions of test PLLA disc. MG-63 cells on both regions have abundant filods (a, b). By contrast, the NIH-3T3 cells have relatively thin, continuous monolayers (c, d). No obvious differences in surface topography were noted comparing the left and right regions.

affected the residual birefringence patterns in sample discs.[25] In this study, we found that the residual stresses in PLLA samples, which developed due to nonuniform cooling, can also be determined by birefringence measurement (Figs. 5a and 5b).

Apart from thermal effects, crystallization shrinkage can also contribute to residual stress development in the injection-molded article. In this study, however, all test regions of the PLLA samples demonstrated amorphous structure without obvious crystallinity peaks (Fig. 4). It appears reasonable to assume, therefore, that, in terms of strain development, the effect of crystallization shrinkage is very low compared to thermal effect.

To identify the mechanisms that underlie cellular sensitivity to various mechanical environments, both silicone rubber and polyacrylamide substrates have been developed for cell culture study.[4,10,12,19,30] However, nondestructive residual stress analysis for both materials is hard to perform. In contrast, the injection-molded PLLA used in this study provided several important benefits: (i) reproducibility of residual stress patterns in the sample discs; (ii) highly sensitive photoelastic properties that could be used for identification and observation of residual internal stress nondestructively; (iii) PLLA is a biomaterial with excellent biocompatibility, providing a physiologically favorable environment for cell growth. However, although PLLA is a biomaterial that serves as a biodegradable scaffold in tissue reengineering and remodeling,[1,16,26] the growth rates of cells seeded on PLLA substrate can still be improved (Fig. 8). Although we found differences in cell distributions of NIH-3T3 and MG-63 at 48 h in the PLLA substrates (Fig. 6), statistically differences in MTT counts was found only in MG-63 but not in NIH-3T3 cultures at this time point (Fig. 8). Accordingly, we can clarify that cell distribution differences between areas on the PLLA surfaces should not be related to the substrate's chemical composition.

Apart from strain-related variants, surface topography characteristics, roughness, and crystallinity may also affect cell behavior. In this study, SEM, WAXRD, and STM were used to control for all these variants. SEM revealed no obvious differences in substrate topography characteristics (Fig. 9). In addition, although geometric roughness (2.3–2.7 μm) was observed on the surface of all the PLLA discs, no significant differences were demonstrated comparing the various test regions. Zinger *et al.*, found that MG63 cells showed minimal responsiveness to surface cavities with diameters lower than 10 μm.[37] It appears

reasonable to assume, therefore, that any surface irregularities on our PLLA discs should not have contributed to variations in cellular distribution.

The crystallinity of polymeric biomaterial is another principle factor influencing cell attachment and proliferation. However, the effects of crystallinity on cell behavior remain controversial. Although fibroblast investigation has demonstrated lower growth rates on crystalline substrates,[17] Zhao *et al.*, found superior cellular attachment on dense highly crystalline surfaces compared to looser less crystalline analogs.[36] In this study, injection of PLLA (melting temperature 185 °C) resulted in uniformly amorphous disc structure. WAXRD testing revealed no significant crystallinity peak can be found among the observed zones (Fig. 4), suggesting the changes in cell distribution on the PLLA are decoupled from this factors.

It has been demonstrated that proliferation of smooth muscle cells cultured on PLA scaffold is strongly affected by residual stresses of their substrate.[26] Using injection-molded method for developing residual stress gradient-PLLA, we confirmed that cell are extremely sensitive to residual stress. Strong relationships were demonstrated between residual stress and cell distribution for both fibroblasts and osteoblastic cells (Fig. 7). Mechanosensing behavior in fibroblasts has been reported when the internal substrate stress reaches 3 kPa.[33] These residual stresses can approach 5 MPa in injection-molded polymethylmethacrylate (PMMA).[35] The Young's modulus of the PLLA used in this study (3 GPa) is close to that of PMMA (2.8 GPa).[18] Although quantitative measurement of residual stresses in the PLLA disc was not performed in this study, it appears reasonable to suggest that the residual stress in injection-molded PLLA is sufficient to produce cellular mechanosensing.

Mechanotransduction may account the explanation for the relationship between residual stress and cell distribution. Cell movement is reportedly the result of traction forces exerted on the substrate via adhesion sites that interface with the cytoskeleton.[12] The relation between cell moving and subtract stiffness is now known as ''durotaxis'' which refered to the phenomenon that the scaffold should have appropriate stiffness to support the cell local motion.[9,14,21] Higher surface stiffness may lead to configuration changes in the membrane protein, which provides physical linkage between the cytoplasm and the substrate.[30] This triggers a downstream signal-transduction cascade, resulting in altered cell behavior. This may also account for the greater cellular spread, elongation,[10] and expression of adhesion-related proteins in cultures on stiffer substrates.[4] Decreasing the residual strain will increase the elastic modulus of the material, resulting in increased traction forces, which provide a force pulling the cell forward.[14] This accounts for the greater cellular accumulation in lower residual-stress regions shown in our study.

The majority of the stiffness modulations are at the ultrastructural level.[21] It is becoming clear that cells can react to the changes in nano-topography on substrate surface using filopodia.[6,7] Although small topographic and chemical differences in nano-scale were not measurement in this study, the residual stresses arising in the PLLA must result in small-scale strain on its surface. This can explain our findings that cells are sensitive to the stress status of their surroundings. The other limitation of this study is to discuss the relevance of our result in 3D scaffolds. Although cells in 2D cultures differ in behavior and integrins expression from those in the 3D environment,[2,5] we suggest that the stress sensing behavior of the cells cultured in the two environments should be the same. This is because stress induced in a material is strongly related to its stiffness which is a basic mechanical property for both 2D and 3D substrates.

CONCLUSION

Based on our limited results, it appears reasonable to suggest that the photoelastic method may provide effective measurement of residual stress in injection-molded PLLA; however, more advanced investigation is needed to clarify the precise mechanisms underlying this behavior. In addition, measurement of cell density indicates that cell growth on PLLA surfaces is affected by residual stress within the substrate. To our knowledge, this is the first demonstration of cellular responsiveness to gradient residual stress.

REFERENCES

[1]Barbanti, S. H., A. R. Santos, Jr., C. A. C. Zavglia, and E. A. R. Duek. Porous and dense poly(L-lactic acid) and poly(D,L-lactic acid-co-glycolic acid) scaffolds: *in vitro* degradation in culture medium and osteoblasts culture. *J. Mater. Sci. Mater. Med.* 15:1315–1321, 2004.

[2]Beningo, K. A., M. Dembo, and Y. Wang. Responses of fibroblasts to anchorage of dorsal extracellular matrix receptors. *PNAS* 101:18024–18029, 2004.

[3]Chaudhry, H. R., B. Bukiet, T. Findley, and A. B. Ritter. Evaluation of residual stress in rabbit skin and relevant material constants. *J. Theor. Biol.* 192:191–195, 1998.

[4]Collin, O., P. Tracqui, A. Stephanou, Y. Usson, J. Clement-Lacroix, and E. Planus. Spatiotemporal dynamics of actin-rich adhesion microdomains: influence of substrate flexibility. *J. Cell Sci.* 119:1914–1925, 2006.

[5]Cukierman, E., R. Pankov, D. R. Stevens, and K. M. Yamada. Taking cell-matrix adhesions to the third dimension. *Science* 294:1708–1712, 2001.

[6]Dalby, M. J., D. Giannaras, M. O. Riehle, N. Gadegaard, S. Affrossmanb, and A. S. G. Curtis. Rapid fibroblast adhesion to 27 nm high polymer demixed nano-topography. *Biomaterials* 25:77–83, 2004.
[7]Dalby, M. J., M. O. Riehle, H. Johnstone, S. Affrossman, and A. S. G. Curtis. Investigating the limits of filopodial sensing: a brief report using SEM to image the interaction between 10 nm high nano-topography and fibroblast filopodia. *Cell Biol. Int*. 28:229–236, 2004.
[8]Dally, J. W., and W. F. Riley. Experimental Stress Analysis. New York: McGraw-Hill, pp. 559–560, 1991.
[9]Discher, D. E., P. Janmey, and Y. Wang. Tissue cells feel and respond to the stiffness of their substrate. *Science* 310:1139–1143, 2005.
[10]Engler, A. J., M. A. Griffin, S. Sen, C. G. Bonnemann, H. E. Sweeney, and D. E. Sischer. Myotubes differentiate optimally on substrate with tissue-like stiffness: pathological implications for soft or stiff microenvironments. *J. Cell Biol*. 166:877–887, 2004.
[11]Isama, K., and T. Tsuchiya. Enhancing effect of poly(L-lactide) on the differentiation of mouse osteoblast-like MC3T3-E1 cells. *Biomaterials* 24:3303–3309, 2003.
[12]Kaverina, I., O. Krylyshkina, K. Beningo, K. Anderson, Y. Wang, and J. V. Small. Tensile stress stimulates microtubule outgrowth in living cells. *J. Cell Sci*. 115:2283–2291, 2002.
[13]Liu, H. C., I. C. Lee, J. H. Wang, S. H. Yang, and T. H. Young. Preparation of PLA membranes with different morphologies for culture of MG-63 cells. *Biomaterials* 25:4047–4056, 2004.
[14]Lo, C. M., H. B. Wang, M. Dembo, and Y. Wang. Cell movement is guided by the rigidity of the substrate. *Biophys. J*. 79:144–152, 2000.
[15]Meredith, J. C., J. L. Sormana, B. G. Keselowsky, A. J. Garcıia, T. Tona, A. Karim, and E. J. Amis. Combinatorial characterization of cell interactions with polymer surfaces. *Biomed. Mater. Res*. 66A:483–490, 2003.
[16]Mikos, A. G., G. Sarakinos, M. D. Lyman, D. E. Ingber, J. P. Vacanti, and R. Langer. Prevascularization of porous biodegradable polymers. *Biotech. Bioeng*. 42:716–723, 1993.
[17]Park, A., and L. G. Cima. *In vitro* cell response to differences in poly-L-lactide crystallinity. *J. Biomed. Mater. Res*. 31:117–130, 1996.
[18]Park, J. B., and R. S. Lakes. Characterization of materials. In: Biomaterials: An Introduction, edited by J. B. Park and R. S. Lakes. New York: Plenum Press, 1992, pp. 63–77.
[19]Pelham, R. J., Jr., and Y. Wang. Cell locomotion and focal adhesions are regulated by substrate flexibility. *Proc. Natl. Acad. Sci. USA* 94:13661–13665, 1997.
[20]Raghavan, M. L., S. Trivedi, A. Nagaraj, D. D. McPherson, and K. B. Chandran. Three-dimensional finite element analysis of residual stress in arteries. *Ann. Biomed. Eng*. 32:257–263, 2004.
[21]Rajagopalan, S., and R. A. Robb. Schwarz meets Schwann: design and fabrication of biomorphic and durataxic tissue engineering scaffolds. *Med. Image Anal*. 10:693–712, 2006.
[22]Rodriguez, E. K., J. H. Omens, L. K. Waldman, and A. D. McCulloch. Effect of residual stress on transmural sarcomere length distributions in rat left ventricle. *Am. J. Physiol*. 264:H1048–H1056, 1993.
[23]Ruimerman, R., B. Van Riebergen, P. Hilbers, and R. Huiskes. The effects of trabecular-bone loading variables on the surface signaling potential for bone remodeling and adaptation. *Ann. Biomed. Eng*. 33:71–78, 2005.
[24]Saunders, M. M., A. F. Taylor, C. Dua, Z. Zhou, V. D. Pellegrini, Jr., and H. J. Donahue. Mechanical stimulation effects on functional end effectors in osteoblastic MG-63 cells. *J. Biomech*. 39:1419–1427, 2006.
[25]Shindo, Y., M. Saito, Y. Iwatsuka, and H. Hasegawa. Residual birefringence of amorphous polymers for optical-disk substrates. *J. Appl. Polym. Sci*. 43:767–773, 1991.
[26]Stitzel, J. D., K. J. Pawloski, G. E. Wnek, D. G. Simpson, and G. L. Bowlin. Arterial smooth muscle cell proliferation on a novel biomimicking, biodegradable vascular graft scaffold. *J. Biomater. Appl*. 16:22–33, 2001.
[27]Subramanian, A., and H. Y. Lin. Crosslinked chitosan: its physical properties and the effects of matrix stiffness on chondrocyte cell morphology and proliferation. *J. Biomed. Mater. Res*. 75A:742–753, 2005.
[28]Tadano, S., and T. Okoshi. Residual stress in bone structure and tissue of rabbit's tibiofibula. *Bio-Med. Mater. Eng*. 16:11–21, 2006.
[29]Vogel, V., and M. Sheetz. Local force and geometry sensing regulate cell functions. *Nature Rev. Mol. Cell Biol*. 7:265–275, 2006.
[30]Wang, H. B., M. Dembo, and Y. Wang. Substrate flexibility regulates growth and apoptosis of normal but not transformed cells. *Am. J. Physiol. Cell Physiol*. 279:C1345–C1350, 2000.
[31]Wang, J. H. C., and B. P. Thampatty. An introductory review of cell mechanobiology. *Biomech. Model. Mechanobiol*. 5:1–16, 2006.
[32]Washburn, N. R., K. M. Yamada, C. G. Simon, Jr., S. B. Kennedy, and E. J. Amis. High-throughput investigation of osteoblast response to polymer crystallinity: influence of nanometer-scale roughness on proliferation. *Biomaterials* 25:1215–1224, 2004.
[33]Yeung, T., P. C. Georges, L. A. Flanagan, B. Marg, M. Ortiz, M. Funaki, N. Zahir, W. Ming, V. Weaver, and P. A. Janmey. Effects of substrate stiffness on cell morphology, cytoskeletal structure, and adhesion. *Cell Motil. Cytoskeleton* 60:24–34, 2005.
[34]Yoon, Y. J., S. H. Jang, G. W. Hwang, and K. W. Kim. Stress distribution produced by correction of the maxillary second molar in buccal crossbite. *Angle Orthod*. 72:397–401, 2002.
[35]Zhao, W., S. Barsun, K. Ramani, T. Johnson, R. King, and S. Lin. Development of PMMA-precoating metal prostheses via injection molding: residual stresses. *J. Biomed. Mater. Res*. 58:456–462, 2001.
[36]Zhao, L., J. Chang, and W. Zhai. Effect of crystallographic phases of TiO_2 on hepatocyte attachment, proliferation and morphology. *J. Biomater. Appl*. 19:237–251, 2005.
[37]Zinger, O., K. Anselme, A. Denzer, P. Habersetzer, M. Wieland, J. Jeanfils, P. Hardouin, and D. Landolt. Time-dependent morphology and adhesion of osteoblastic cells on titanium model surface featuring scale-resolved topography. *Biomaterials* 25:2695–2711, 2004.